Comparing the spatial patterns of climate change in the 9th and 5th millennia B.P. from TRACE-21 model simulations

Liang Ning[1,2,3], Jian Liu[1,2*], Raymond S. Bradley[3], and Mi Yan[1,2]

[1]Key Laboratory of Virtual Geographic Environment, Ministry of Education; State key Laboratory of Geographical Environment Evolution, Jiangsu Provincial Cultivation Base; School of Geographical Science, Nanjing Normal University, Nanjing, 210023, China

[2]Jiangsu Center for Collaborative Innovation in Geographical Information Resource Development and Application, Nanjing, 210023, China

[3]Climate System Research Center, Department of Geosciences, University of Massachusetts, Amherst, 01003, United States

[*]jliu@njnu.edu.cn

ABSTRACT

The spatial patterns of global temperature and precipitation changes, as well as corresponding large-scale circulation patterns during the latter part of the 9th and 5th millennia B.P. (4800-4500 versus 4500-4000 years B.P. and 9200-8800 versus 8800-8000 years B.P.) are compared through a group of transient simulations using the Community Climate System Model version 3 (CCSM3). Both periods are characterized by significant sea surface temperature decreases over the North Atlantic south of Iceland. Temperatures were also colder across the northern hemisphere, but warmer in the southern hemisphere. Significant precipitation decreases are seen over most of the northern hemisphere, especially over Eurasia and the Asian monsoon regions, indicating a weaker summer monsoon. Large precipitation anomalies over northern South America and adjacent ocean regions are related to a southward displacement of the Inter Tropical Convergence Zone (ITCZ) in that region. Climate changes in the late 9th millennium B.P. ("The 8.2ka BP event ") are widely considered to have been caused by a large fresh water discharge into the northern Atlantic, which is confirmed in a meltwater forcing sensitivity experiment, but this was not the cause of changes occurring between the early and latter half of the 5th millennium B.P. Model simulations suggest that a combination of factors, led by long-term changes in insolation, drove a steady decline in SSTs across the North Atlantic and a reduction in the AMOC, over the past 4500 years, with associated teleconnections across the globe, leading to drought in some areas. Multi-century scale

fluctuations in SSTs and AMOC strength were superimposed on this decline. This helps explain the onset of neoglaciation around 5000-4500 BP, followed by a series of neoglacial advances and retreats during recent millennia. The "4.2ka B.P. event" appears to have been one of several late Holocene multi-century fluctuations that were embedded in the long-term, low frequency change in climate that occurred after ~4.8 ka BP. Whether these multi-century fluctuations were a response to internal centennial-scale ocean-atmosphere variability or external forcing (such as explosive volcanic eruptions and associated feedbacks) or a combination of such conditions, is not known and requires further study.

1. Introduction

It is well-documented that the first order driver of Holocene climate change was orbital forcing, with an overall decline in summer insolation in summer months, particularly at high latitudes. This led to a drop in temperatures at high latitudes and less rainfall throughout the monsoon regions of the northern hemisphere, as seen in many paleoclimatic records (Burns, 2011; Solomina et al., 2015). Shorter-term rainfall fluctuations superimposed on this long-term change in hydrological conditions are clearly seen in many speleothem and lacustrine sediment records (e.g. Wang et al., 2005; Kathayat et al., 2017). Abrupt hydrological changes around 4.2 ka BP have been documented for various regions of the world; it has been suggested that the major global monsoon and ocean-atmosphere circulation systems were deflected or weakened synchronously at this time, causing major century-scale precipitation disruptions (severe megadroughts) over different regions (Weiss, 2017). Other studies (Wang et al., 2005; Tan et al., 2018a) have also noted weakening of the Asian summer monsoon at around this time, resulting in drought over the northern part of eastern China and flooding over the southern part.

In recent years, a more comprehensive picture of the "4.2 ka BP event" has been derived from analysis of new high-resolution proxy data from different regions, and the event has become the focus of symposia and research conferences (e.g. Weiss, 2015). This event is of particular interest as it is associated with societal collapse and regional abandonment in many different regions. For example, the collapse and abandonment of Akkadian imperial settlements in the Khabur Plains, and other communities in dry farming domains across the Aegean and West Asia, was in response to the abrupt nature with which the megadrought began (with its onset in less than

five years), its magnitude (a precipitation reduction of 30-50%) and its long duration (200-300 years) (Weiss, 2017).

Although a drought episode around 4.2ka B.P. has been found in many proxy reconstructions, the mechanisms that brought this about are still unclear, though different hypotheses have been proposed. For example, Staubwasser and Weiss (2006) suggested that the abrupt climate change event at 4.2ka B.P., as well as other widespread droughts around 8.2ka BP and 5.2ka BP over the eastern Mediterranean, West Asia, and the Indian subcontinent, were caused by a change in subtropical upper-level flow over the eastern Mediterranean and Asia. Some studies have suggested that these large-scale circulation anomalies may reflect persistent modes of internal climate variability, though there is a wide range of other explanations. For example, Booth et al. (2005) indicated that the widespread mid-latitude and subtropical drought around 4.2ka BP was linked to a La Niña-like SST pattern, possibly associated with amplification of this spatial mode by variations in solar irradiance or volcanism. On the other hand, Hong et al. (2005) analyzed a 12,000-yr proxy record for the East Asian monsoon and concluded that such abnormal climate conditions could possibly result from frequent and severe El Niño activities. Using paired oxygen isotope records from North America, Liu et al. (2014b) indicated that there was a transition from a negative Pacific North American (PNA)-like pattern during the mid-Holocene to a positive PNA-like pattern during the late Holocene, which led to drier conditions in northwestern North America. A similar conclusion was reached by Finkenbinder et al. (2016) based on lake sediment records from Newfoundland. They argued that this transition took place around 4.3ka B.P., leading to wetter conditions across the Newfoundland region. In contrast, Bond et al. (2001) argued that North Atlantic SST anomalies around 4.2ka B.P. were related to a negative North Atlantic Oscillation (NAO) pattern, linked to solar forcing. Deininger et al. (2017) also found that changes in the atmospheric circulation associated with northward and southward propagating westerlies (similar to the NAO but on a millennial instead of a decadal scale) could be a possible driver of coherency and cyclicity during the last 4.5ka BP, as seen in multiple speleothem $\delta^{18}O$ records that span most of the European continent. Thus, although there have been many suggested mechanisms, the ultimate drivers for climatic anomalies at 4.2ka B.P. remain unclear.

Wang (2009a) reviewed studies of Holocene cold events, and concluded that the most severe Holocene cold event, at ~8.2ka BP, was brought about by an outburst flood from pro-glacial Lake Agassiz. This large volume of freshwater drained into the North Atlantic extremely rapidly,

leading to a brief reorganization of the North Atlantic Meridional Overturning Circulation (AMOC) and a southward displacement of the ITCZ, resulting in dry conditions over many regions (Barber et al., 1999; Bianchi and McCave, 1999; Risebrobakken et al., 2003; McManus et al., 2004; Clarke et al., 2004). Potential external forcing factors for the 4.2ka BP event include non-linear responses to Milankovitch forcing, solar irradiance variations, and explosive volcanic eruptions, all of which may have brought about variations in the ocean-atmosphere system (Booth et al., 2005). Wang (2009a) concluded that solar irradiance minima were the main cause of cold events in the mid- to late Holocene (including the 4.2ka BP event) and that internal oscillations within the climate system could possibly have intensified these cold events under certain circumstances (Wang, 2009b).

In summary, the 8.2ka BP event and corresponding southward shift in the ITCZ were caused by glacial flooding of the North Atlantic and this can be reasonably simulated by coupled GCMs with different boundary conditions and freshwater forcing (Alley and Agustsdottir, 2005; LeGrande et al., 2006). By contrast, the forcing mechanisms that brought about the 4.2ka BP event are currently uncertain. At 4.2ka B.P., the major global monsoon and ocean-atmosphere circulation systems may have been deflected or weakened synchronously, causing major century-scale precipitation disruptions, with severe megadroughts over many different regions (Weiss, 2017). As GCM simulations of the 4.2ka BP event have not received much attention, in this study, the spatial patterns and corresponding mechanisms relevant to the 4.2 ka BP event are examined and compared to those associated with the 8.2ka BP event.

2. Data and methodology

Simulations of the last 21ka (TRACE-21) were used in this study (He, 2011; He et al. 2013; Wen et al., 2016). These transient simulations have been completed using Version 3 of the Community Climate System Model (CCSM3), which is a coupled atmosphere-ocean general circulation model developed by the National Center for Atmospheric Research (NCAR). The atmosphere model in the CCSM3 is the Community Atmospheric Model 3 (CAM3) with a horizontal resolution of ~3.75° (T31), and the ocean model is the Parallel Ocean Program (POP) with a longitudinal resolution of 3.6° and variable latitudinal resolution.

The "full-forcing" TRACE-21 simulation includes changes in orbital parameters, greenhouse gases, ice extent (based on the ICE 5G-VM2 configurations) and meltwater fluxes from the

Northern Hemisphere and Antarctic ice sheets. The orbital forcing is based on transient variations of orbital configuration (Berger, 1978). The concentrations of greenhouse gases were adopted from Joos and Spahni (2008). The ice sheet data were modified from the reconstruction of Peltier (2004) and the meltwater scheme was adopted from Liu et al. (2009).

Simulations in which only one of these factors was included have also been carried out and are available in the TRACE-21 archive (Otto-Bliesner et al., 2006; Wen et al., 2016). These simulations can reproduce the timing and magnitude of many aspects of climate evolution during the last 21 ka, such as changes in sea surface temperature (SST) (He et al., 2013). However, there are significant differences between the rate of temperature change in the model during the early Holocene and many paleoclimatic records (Liu et al., 2014a; Marcott et al., 2013; Marsicek et al., 2018). In this study, we do not address this enigma, but use the transient model data to compare intervals within the Holocene when abrupt changes in climate are known to have occurred in some regions (~8.2ka B.P. and ~4.2ka B.P.). These times were recently adopted by the International Commission on Stratigraphy as the chronological boundaries of the early, mid and late Holocene (Walker et al., 2012, 2018).

We examine mean annual surface temperature, annual precipitation and SSTs from the full-forcing experiment, and also AMOC strength, defined as the maximum Atlantic stream function between 20-50°N between 500m and 5000m depth (Ottera et al., 2010) from the full-forcing and orbital-forcing experiments.

3. Results

First, we assess Holocene climate variability as simulated in the full-forcing experiment. Fig. 1 shows the time series of surface temperature and precipitation over the last past 13ka. It shows cooling associated with the Younger Dryas, followed by Holocene warming, but also a brief cooling episode from ~8500-8000 B.P. Thereafter the record exhibits strong multi-century scale variability. Temperature and precipitation are positively correlated at this global scale. It is tempting to associate the colder episodes with those identified by Wanner et al (2011) or by Bond et al. (2001) but only a few of these are coincident in time.

The period 4.5ka-4.0ka BP was chosen for analysis, by subtracting the mean annual 2m air temperatures, SSTs and precipitation of the period 4500-4000 years B.P. from the preceding period (4800-4500 years B.P.). The spatial distribution of air temperature (Fig. 2a) shows that

temperatures were significantly colder over most of the extra-tropical northern hemisphere, but generally warmer in the Tropics and in the southern hemisphere. The main exceptions are northern South America, which was cooler, and northern India and Pakistan, which were significantly warmer. Precipitation decreased over almost all of the northern hemisphere, particularly in the Tropics where the ITCZ shifted southward, mainly over South America and adjacent ocean regions, resulting in higher rainfall in the 0-20ºS zonal band from 4500-4000 years B.P. (Figure 2b). There was less precipitation over the northern part of China but more precipitation over southern China, consistent with paleoclimate reconstructions that indicate a weaker East Asian monsoon (Wang et al., 2005; Tan et al., 2018a). This pattern is also similar to the situation during the LIA in China and some of the megadroughts that have happened in recent centuries (Cook et al., 2010; Tan et al., 2018b). Over other Asian monsoon regions, such as India, there were also significant precipitation reductions during the second half of the 5th millennium B.P., consistent with speleothem records that show a decline in Indian summer monsoon rainfall over this period (Kathayat et al., 2017). Over Central America and the northern edge of South America, conditions were also drier in the later period, but over the rest of South America, and adjacent ocean regions, precipitation was higher, due to a southward displacement of the ITCZ; this pattern is supported by speleothem records of rainfall in Mexico and Brazil (Lachniet et al., 2013; Bernal et al., 2016). The SST pattern shows significantly cooler temperatures in the period 4500-4000years B.P. over the North Atlantic. This cooling is centered around 50°N (south of Iceland) and extends into the sub-Tropics on the eastern side of the sub-tropical gyre. Slightly cooler temperatures are also found over the North Pacific (Fig. 2c). By contrast, for most of the southern hemisphere there was a positive change in temperature. Rotated EOF analysis on the global SST field shows the primary feature (in EOFs 1 and 2) to be the cooler SSTs over the North Atlantic, with a shift around 4.5ka BP from a predominantly positive to a generally negative pattern (Fig. 3). This is similar to an AMO-like pattern over the northern Atlantic that has been identified in both instrumental and paleoclimatic records (Delworth and Mann, 2000; Knudsen et al., 2011).

The same evaluation of changes in the 9th millennium B.P. was made by subtracting the mean annual 2m air temperatures, SSTs and precipitation from 8800-8000 from the preceding period (9200-8800 years B.P.), since an abrupt change in temperature in the model occurred around 8.8 ka BP (Fig. 1a). Air temperatures were significantly lower in the second period over most of the northern hemisphere; only a zone from northern South America across to sub-Saharan Africa

and India was warmer in the second period (Fig. 4a). Almost the entire southern hemisphere was warmer. Precipitation was less in the second period across all of the northern hemisphere, especially along the ITCZ, which was displaced to the south. This resulted in increased rainfall in a belt south of the Equator, across almost all of the Tropics (Fig. 4b). The rest of the southern hemisphere was also slightly wetter. SSTs show a strong pattern of cooling over the North Pacific, and the eastern North Atlantic, south of Iceland, extending around the Atlantic sub-tropical gyre into the tropical Atlantic and Caribbean (Fig. 4c). Rotated EOFs show that the anomalies in the North Atlantic and North Pacific dominate the first 3 EOFs (Fig. 5).

The spatial patterns of temperature changes, precipitation changes, and SST changes were remarkably similar in the late 9th millennium and in the period leading up to the late 5th millennium (Fig. 6). The major difference (Fig. 6a) is that SST changes over the subtropical Atlantic were greater, and the related changes across the northern hemisphere in the 9th millennium B.P. were larger, than in the late 5th millennium. Similarly, the major changes in precipitation patterns were comparable, but less pronounced from 4500-4000 years B.P. These similarities are somewhat puzzling as the meltwater forcing sensitivity experiment clearly shows that the "8.2ka BP event" was induced by a massive freshwater flux into the Atlantic whereas (as far as we know) no comparable meltwater event occurred in the late Holocene so it seems unlikely that such forcing was a factor driving the changes seen in the model output for 4500-4000 years B.P.

4. Discussion and Conclusions

Paleoclimate records have shown that unusually dry conditions persisted for several centuries around 4.2ka BP over many regions, and in some areas these had devastating societal impacts. In this study, the spatial patterns of temperature, precipitation, and corresponding circulation anomalies during the latter part of the 9th and 5th millennia B.P. (4800-4500 versus 4500-4000 years B.P. and 9200-8800 versus 8800-8000 years B.P.) were compared based on model simulations. The changes in climate during both periods were similar and characterized by significant temperature and precipitation decreases over most of the northern hemisphere, whereas the southern hemisphere was slightly warmer and wetter. In particular, the ITCZ was displaced to the south across much of the globe, and monsoon regions of the northern hemisphere were generally drier. On a regional scale, there was less precipitation over the northern part of China but more precipitation over southern China, indicating a reduced eastern Asian summer monsoon.

It is clear that the earlier period was strongly influenced by freshwater forcing in the North Atlantic, which drastically reduced the Atlantic Meridional Overturning Circulation (AMOC). The similarity in anomaly patterns between the 8.2ka BP event and the late 5th millennium BP suggests that there was also disruption to the AMOC in the later period. However, as there was no comparable freshwater forcing in the 5th millennium B.P., we must therefore consider what other factors might have played a role in reducing AMOC strength. There were no major solar irradiance changes at that time, so we can rule that out as a forcing factor. However, there was a major eruption of the Icelandic volcano Hekla at ~4200 BP, and it is possible that such an event could have brought about regional cooling, leading to more extensive, thick sea-ice and attendant freshwater effects on the AMOC (cf. Moreno-Chamarro et al., 2017). This mechanism deserves further scrutiny.

In the "all forcing" TRACE-21 simulation, AMOC strength declined slightly during the late Holocene and underwent multi-century fluctuations (Fig. 7a), which were strongly correlated with SSTs in the region of the North Atlantic where cooling was so prominent from 4.5-4.0 ka B.P. (Fig. 8). Mean SSTs in this region over the last 4500 years of the model simulation stayed below the 4.8-4.5 ka B.P. average for ~69% of the time (Fig. 8), and AMOC strength was similarly below the 4.8-4.5 ka BP mean for 63% of the time (Fig. 7a). One of these fluctuations was associated with an AMOC minima around 4.2ka BP. In the TRACE-21 model simulation with only orbital forcing, AMOC strength reached its Holocene maximum around 4.8 ka BP, then slightly weakened (by ~10%) over the late Holocene, staying below the 4.8-4.5ka BP mean for 87% of the time, with minor multi-century variations superimposed on the long-term downward trend (Fig. 7b). This suggests that a combination of factors, led by long-term changes in insolation, drove a steady decline in SSTs across the North Atlantic and a reduction in the AMOC, with associated teleconnections across the globe (including drought in some regions). Minor fluctuations around this declining trend were the dominant pattern for most of the last 4500 years. This interpretation helps explain widespread paleoclimatic evidence for the onset of neoglaciation around 5000-4500 BP, followed by a series of neoglacial advances and retreats during recent millennia (Porter, 2000; Barclay et al., 2009; Solomina et al., 2015; Bradley and Bakke, 2018). Since the onset of neoglaciation early in the 5th millennium B.P., mountain glaciers fluctuated in extent but did not entirely disappear, indicating that a distinctly different climate state prevailed compared to the period prior to ~5 ka B.P., when many mountain regions were ice-free.

We therefore conclude from the model simulations that the "4.2ka B.P. event" was one of several late Holocene multi-century fluctuations that were embedded in a long-term, low frequency change in climate that occurred after ~4.8 ka BP. World-wide climatic anomalies during these fluctuations were driven by changes in the strength of the AMOC and related teleconnections. Whether such multi-century fluctuations were a response to internal centennial-scale ocean-atmosphere variability (cf Min and Liu, 2018), or external forcing (such as explosive volcanic eruptions and associated feedbacks) or a combination of such conditions, is not known. Further studies of the role of both external forcing and internal variability are needed to provide a better understanding of such mechanisms (cf. Ottera et al., 2010; Moreno-Chamarro et al., 2017; Gupta and Marshall, 2018).

Acknowledgements

This research was jointly supported by the National Key Research and Development Program of China (Grant No.2016YFA0600401), the National Natural Science Foundation of China (Grant No. 41501210, Grant No. 41420104002, Grant No. 41671197, and Grant No. 41631175), the Jiangsu Province Natural Science Foundation (Grant No. BK20150977), Top-notch Academic Programs Project of Jiangsu Higher Education Institutions (Grant No. PPZY2015B115), and the Priority Academic Development Program of Jiangsu Higher Education Institutions (Grant No. 164320H116). Support was alo received from U.S. NSF grant PLR-1417667 to the University of Massachusetts. TraCE-21ka was made possible by the DOE INCITE computing program, and supported by NCAR, the NSF P2C2 program, and the DOE Abrupt Change and EaSM programs.

References:

Alley, R.B., and Agustsdottir, A.M.: The 8k event: cause and consequences of a major Holocene abrupt climate change. *Quaternary Science Reviews*, 24, 1123–1149, 2005.

Barber, D.C., Dyke, A., Hillaire-Marcel, C., Jennings, A.E., Andrews, J.T., Kerwin, M.W., Bilodeau, G., McNeely, R., Southon, J., Morehead, M.D. and Gagnon, J.M.: Forcing of the cold event of 8,200 years ago by catastrophic drainage of Laurentide lakes. *Nature*, 400 (6742), 344-348, 1999.

Barclay, D.J., Wiles, G.C. and Calkin, P.E.: Holocene glacier fluctuations in Alaska. *Quaternary Science Reviews*, 28 (21-22), 2034-2048, 2009.

279 Berger, A. L. Long-term variations of daily insolation and Quaternary climatic changes. *J. Atmos.*
280 *Sci*. 35, 2362–2367, 1978.
281 Bernal, J.P., Cruz, F.W., Stríkis, N.M., Wang, X., Deininger, M., Catunda, M.C.A., Ortega-
282 Obregón, C., Cheng, H., Edwards, R.L. and Auler, A.S.: High-resolution Holocene South
283 American monsoon history recorded by a speleothem from Botuverá Cave, Brazil. *Earth and*
284 *Planetary Science Letters,* 450, 186-196, 2016.
285 Bianchi, G., and McCave, I.N.: Holocene periodicity in north Atlantic climate and deep ocean flow
286 south of Iceland. *Nature*, 397, 515–518, 1999.
287 Bond, G., Kromer, B., Beer, J., Muscheler, R., Evans, M.N., Showers, W., Hoffmann, S., Lotti-
288 bond, R., Hajdas, I. and Bonani, G.: Persistent solar influence on North Atlantic climate during
289 the Holocene. *Science,* 294, 2130-2136, 2001.
290 Booth, R. K., Jackson, S. T., Forman, S. L., Kutzbach, J. E., Bettis III, E. A., Kreig, J., and Wright,
291 D. K.: A severe centennial-scale drought in mid-continental North America 4200 years ago and
292 apparent global linkage. *The Holocene*, 15, 321-328, 2005.
293 Bradley, R.S. and Bakke, J., Is there evidence for a 4.2ka BP event in the northern North Atlantic
294 region? *Climate of the Past Discussions* (in review), 2018.
295 Burns, S.J.: Speleothem records of changes in tropical hydrology over the Holocene and possible
296 implications for atmospheric methane. *The Holocene*, 21, 735-741, 2011.
297 Clarke, G.K.C., Leverington, D.W., Teller, J.T., and Dyke, A.S.: Paleohydraulics of the last
298 outburst flood from glacial Lake Agassiz and the 8200 BP cold event. *Quaternary Science*
299 *Reviews*, 23, 389–407, 2004.
300 Cook, E. R., Anchukaitis, K. J., Buckley, B. M., D'Arrigo, R. D., Jacoby, G. C., and Wright, W.
301 E.: Asian monsoon failure and megadrought during the last millennium. *Science*, 328, 486-489,
302 2010.
303 Deininger, M., McDermott, F., Mudelsee, M., Werner, M., Frank, N., Mangini, A.: Coherency of
304 late Holocene European speleothem $\delta^{18}O$ records linked to North Atlantic Ocean circulation.
305 *Climate Dynamics*, 49, 595-618, 2017.
306 Delworth, T.L. and Mann, M.E.: Observed and simulated multidecadal variability in the Northern
307 Hemisphere, Climate Dynamics, 16, 661-676, 2000.
308 Finkenbinder, M. S., Abbott, M. B., and Steinman, B. A.: Holocene climate change in
309 Newfoundland reconstructed using oxygen isotope analysis of lake sediment cores. *Global and*

Planetary Change, 143, 251-261, 2016.

Gupta, M. and Marshall, J.: The climate response to multiple volcanic eruptions mediated by ocean heat uptake: damping processes and accumulation potential. *J. Climate*, 31, 8669-8687, 2018.

He, F.: *Simulation transient climate evolution of the last deglaciation with CCSM3*. PhD dissertation, University of Wisconsin-Madison, 185pp, 2011.

He, F., Shakun, J. D., Clark, P. U., Carlson, A. E., Liu, Z., Otto-Bliesner, B. L., and Kutzbach J. E.: Northern Hemisphere forcing of Southern Hemisphere climate during the last deglaciation. *Nature*, 494, 81-85, 2013.

Joos, F., and Spahni, R.: Rates of change in natural and anthropogenic radiative forcing over the past 20,000 years, *Proceedings of the National Academy of Sciences, 105*, 1425-1430, doi: 10.1073/pnas.0707386105, 2008.

Kathayat, G., Cheng, H., Sinha, A., Yi, L., Li, X., Zhang, H., Li, H., Ning, Y. and Edwards, R.L.: The Indian monsoon variability and civilization changes in the Indian subcontinent. *Science Advances*, 3, e1701296, 2017.

Knudsen, M.F., Seidenkrantz, M.S., Jacobsen, B.H. and Kuijpers, A.: Tracking the Atlantic Multidecadal Oscillation through the last 8,000 years. *Nature Communications*, 2, 178-185, 2011.

Lachniet, M.S., Asmerom, Y., Bernal, J.P., Polyak, V.J. and Vazquez-Selem, L.: Orbital pacing and ocean circulation-induced collapses of the Mesoamerican monsoon over the past 22,000 y. *Proceedings of the National Academy of Sciences*, 110, 9255-9260, 2013.

LeGrande, A.N., Schmidt, G.A., Shindell, D.T., Field, C.V., Miller, R.L., Koch, D.M., Faluvegi, G. and Hoffmann, G.: Consistent simulations of multiple proxy responses to an abrupt climate change event. *Proceedings of the National Academy of Sciences*, 103, 837–842, 2006.

Liu, Z., Otto-Bliesner, B.L., He, F., Brady, E.C., Tomas, R., Clark, P.U., Carlson, A.E., Lynch-Stieglitz, J., Curry, W., Brook, E. and Erickson, D.: Transient simulation of last deglaciation with a new mechanism for Bølling-Allerød warming. *Science*, *325* (5938), 310-314, 2009.

Liu, Z., Zhu, J., Rosenthal, Y., Zhang, X., Otto-Bliesner, B.L., Timmermann, A., Smith, R.S., Lohmann, G., Zheng, W. and Timm, O.E.: The Holocene temperature conundrum. *Proceedings of the National Academy of Sciences*, 111, E3501-E3505, 2014a.

Liu, Z., Yoshimura, K., Bowen, G. J., Buenning, N. H., Risi, C., Welker, J. M., and Yuan, F.:

Paired oxygen isotope records reveal modern North American atmospheric dynamics during the Holocene. *Nature Communications*, 5, 3701, DOI: 10.1038/ncomms4701, 2014b.

Marsicek, J., Shuman, B.N., Bartlein, P.J., Shafer, S.L. and Brewer, S.: Reconciling divergent trends and millennial variations in Holocene temperatures. *Nature*, 554 (7690), 92-96, 2018.

Marcott, S.A., Shakun, J.D., Clark, P.U., and Mix, A.C.: A reconstruction of regional and global temperature for the past 11,300 years. *Science*, 339, 1198-1201, 2013.

McManus, J.F., Francois, R., Gherardi, J.-M., Keigwin, L. D., and Brown-Leger, S.: Collapse and rapid resumption of Atlantic meridional circulation linked to deglacial climate changes. *Nature*, 428, 834–837, 2004.

Moreno-Chamarro, E., Zanchettin, D., Lohmann, K and Jungclaus, J.H., An abrupt weakening of the subpolar gyre as trigger of Little Ice Age-type episodes. *Climate Dynamics*, 48, 727-744, 2017.

Ottera, O. H., Bentsen, M., Drange, H., and Suo, L.: External forcing as a metronome for Atlantic multidecadal variability. *Nature Geoscience*, 3, 688-694, 2010.

Otto-Bliesner, B. L., Brady, E. C., Clauzet, G., Tomas, R., Levis, S., and Kothavala, Z.: Last Glacial Maximum and Holocene climate in CCSM3. *J. Climate*, 19, 2526-2544, 2006.

Peltier, W. R.: Global glacial isostasy and the surface of the ice-age Earth-The ICE-5G (VM2) model and GRACE, *Annual Rev. Earth Planet. Sci., 32*, 111-149, 2004.

Porter, S.C.: Onset of neoglaciation in the Southern Hemisphere. *Journal of Quaternary Science*, 15 (4), 395-408, 2000

Risebrobakken, B., Jansen, E., Andersson, C., Mjelde, E., Hevrøy, K.: A high resolution study of Holocene paleoclimatic and paleoceanographic changes in the Nordic Seas. *Paleoceanography*, 18, 1–14, 2003.

Solomina, O.N., Bradley, R.S., Hodgson, D.A., Ivy-Ochs, S., Jomelli, V., Mackintosh, A.N., Nesje, A., Owen, L.A., Wanner, H., Wiles, G.C. and Young, N.E.: Holocene glacier fluctuations. *Quaternary Science Reviews*, 111, 9-34, 2015.

Staubwasser, M., and Weiss, H.: Holocene climate and cultural evolution in late prehistoric-early historic West Asia. *Quaternary Research*, 66, 372-387, 2006.

Tan, L., Cai, Y., Cheng, H., Edwards, L. R., Gao, Y., Xu, H., Zhang, H., and An, Z.: Centennial- to decadal- scale monsoon precipitation variations in the upper Hanjiang River region, China over the past 6650 years. *Earth and Planetary Science Letters*, 482, 580-590, 2018a.

372 Tan, L., Cai, Y., Cheng, H., Edwards, L. R., Lan, J, Zhang, H., Li, D, Ma, L. Zhao, P. and Gao,
373 Y.: High resolution monsoon precipitation changes on southeastern Tibetan Plateau over the
374 past 2300 years. *Quaternary Science Reviews*, 195, 122-132, 2018b.
375 Walker, M.J., Berkelhammer, M., Björck, S., Cwynar, L.C., Fisher, D.A., Long, A.J., Lowe, J.J.,
376 Newnham, R.M., Rasmussen, S.O. and Weiss, H.: Formal subdivision of the Holocene
377 Series/Epoch: a Discussion Paper by a Working Group of INTIMATE (Integration of ice-core,
378 marine and terrestrial records) and the Subcommission on Quaternary Stratigraphy
379 (International Commission on Stratigraphy). *Journal of Quaternary Science*, 27, 649-659,
380 2012.
381 Walker, M.J., Berkelhammer, M., Björck, S., Cwynar, L.C., Fisher, D.A., Long, A.J., Lowe, J.J.,
382 Newnham, R.M., Rasmussen, S.O. and Weiss, H.: Formal ratification of the subdivision of the
383 Holocene Series/Epoch (Quaternary System/Period): two new Global Boundary Stratotype
384 Sections and Points (GSSPs) and three new stages/subseries. *Episodes*, 41, 2018.
385 Wang, S.: Holocene climate, *Advances in climate change research*, 5, 247-248, 2009a (in Chinese
386 with English abstract)
387 Wang, S.: Holocene cold events in the north Atlantic chronology and climatic impact, *Quaternary*
388 *Sciences*, 29, 1146-1153, 2009b (in Chinese with English abstract)
389 Wang, Y., Cheng, H., Edwards, L. R., He, Y., Kong, X., An, Z., Wu, J., Kelly, M. J., Dykoski, C.
390 A., and Li, X.: The Holocene Asian monsoon: links to solar changes and north Atlantic climate,
391 *Science*, 308, 854-857, 2005.
392 Weiss, H.: Megadrought, collapse, and resilience in late 3rd millennium BC Mesopotamia. In :
393 Meller, H., Arz, H. W., Jung, R., and Risch, R., eds, 2200 BC – *A climatic breakdown as a*
394 *cause for collapse of the Old World?* Halle: Landesmuseum fur Vorgeschichte, 35-52, 2015.
395 Weiss, H.: 4.2ka BP megadrought and the Akkadian collapse. In: Weiss, H., ed., *Megadrought*
396 *and Collapse*, Oxford University Press, 93-159, 2017.
397 Wen, X, Liu, Z, Wang, S. Cheng, J. and Zhu, J.: Correlation and anti-correlation of the East Asian
398 summer and winter monsoons during the last 21,000 years. *Nature Communications*, 7,
399 11999, 2016.
400 Yan, M and Liu, J., Physical processes of cooling and megadrought in 4.2ka BP event: results from
401 TRACE-21 simulations. *Climate of the Past Discussions* (in review), 2018

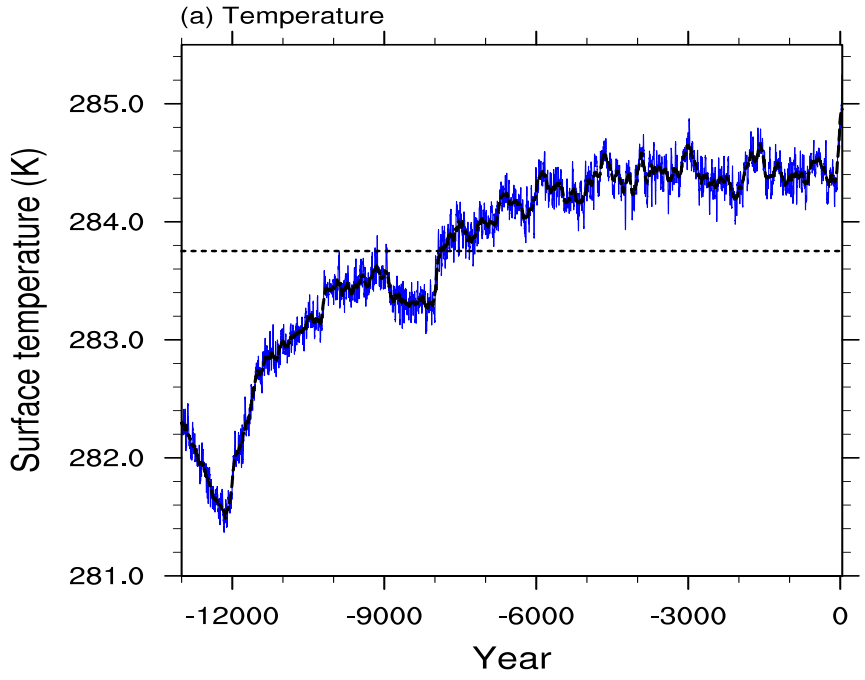

402

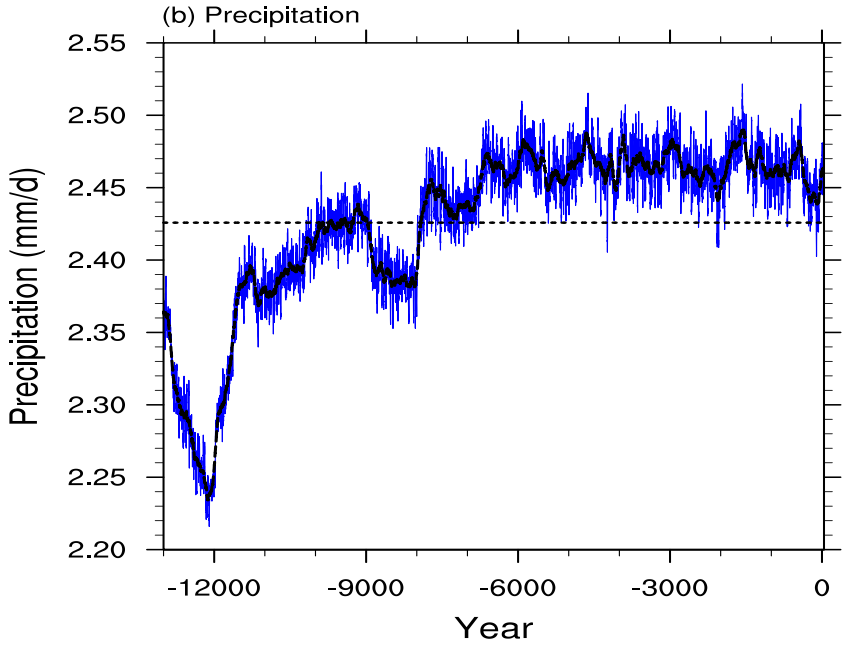

403
404
405

406 **Figure 1**. (a) Northern hemisphere average surface temperature and (b) precipitation over the last
407 13ka years from the all-forcing experiment. Blue line is the 10-year running average and the black
408 line is the 100-year running average. The black dash line shows the average of the time series.

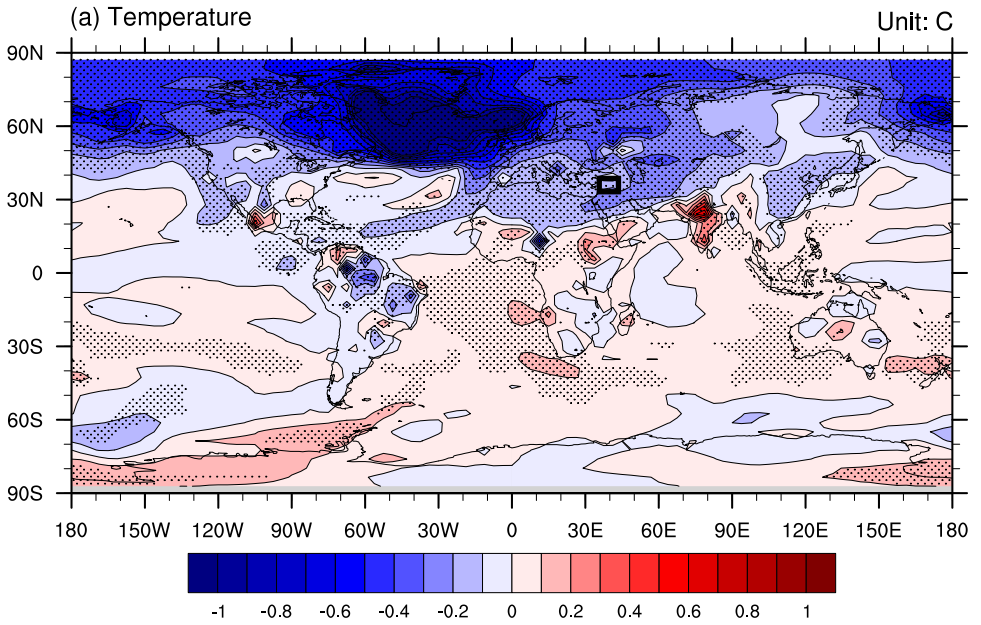
(a) Temperature
Unit: C
90N
60N
30N
0
30S
60S
90S
180 150W 120W 90W 60W 30W 0 30E 60E 90E 120E 150E 180
-1 -0.8 -0.6 -0.4 -0.2 0 0.2 0.4 0.6 0.8 1

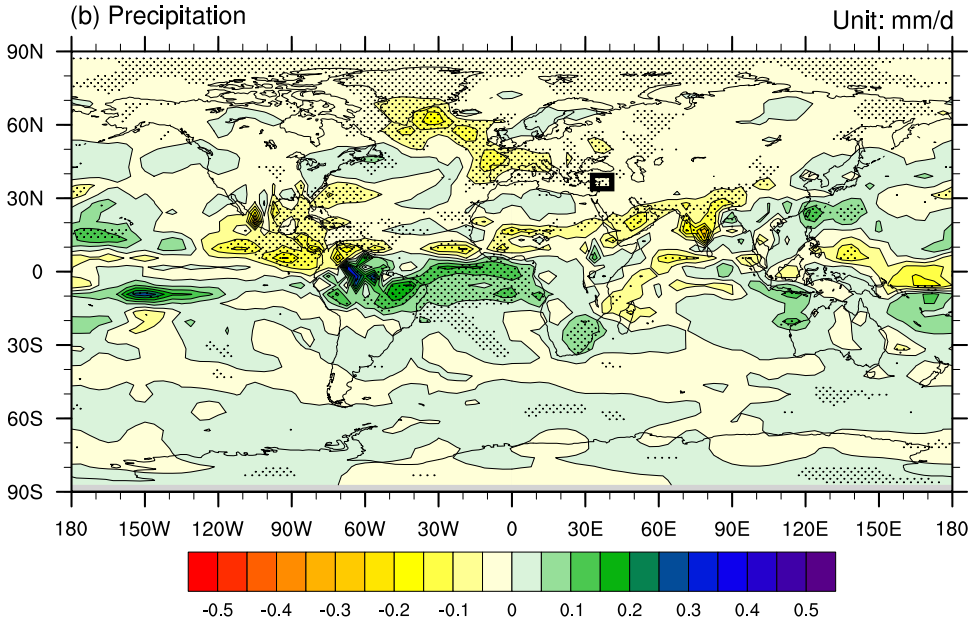
(b) Precipitation
Unit: mm/d
90N
60N
30N
0
30S
60S
90S
180 150W 120W 90W 60W 30W 0 30E 60E 90E 120E 150E 180
-0.5 -0.4 -0.3 -0.2 -0.1 0 0.1 0.2 0.3 0.4 0.5

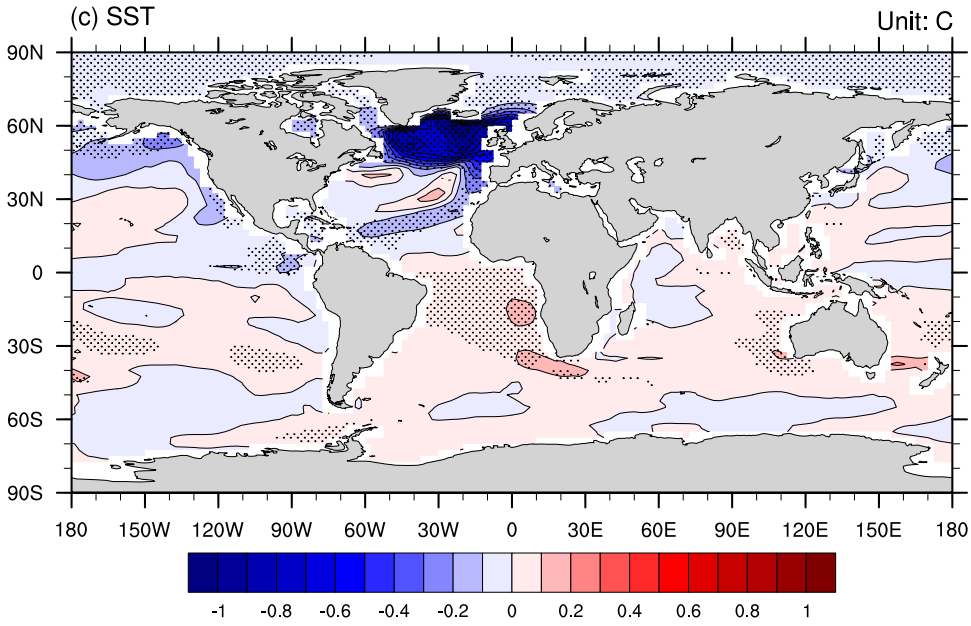

Figure 2. The changes of (a) surface temperature (°C), (b) precipitation (mm/day), and (c) SST (°C) after 4.5ka BP (between 4500-4000ka BP and 4800-4500ka BP). The rectangles in (a) and (b) indicate the region with major dry-farming settlement abandonment around 4.2ka BP, according to Weiss (2016).

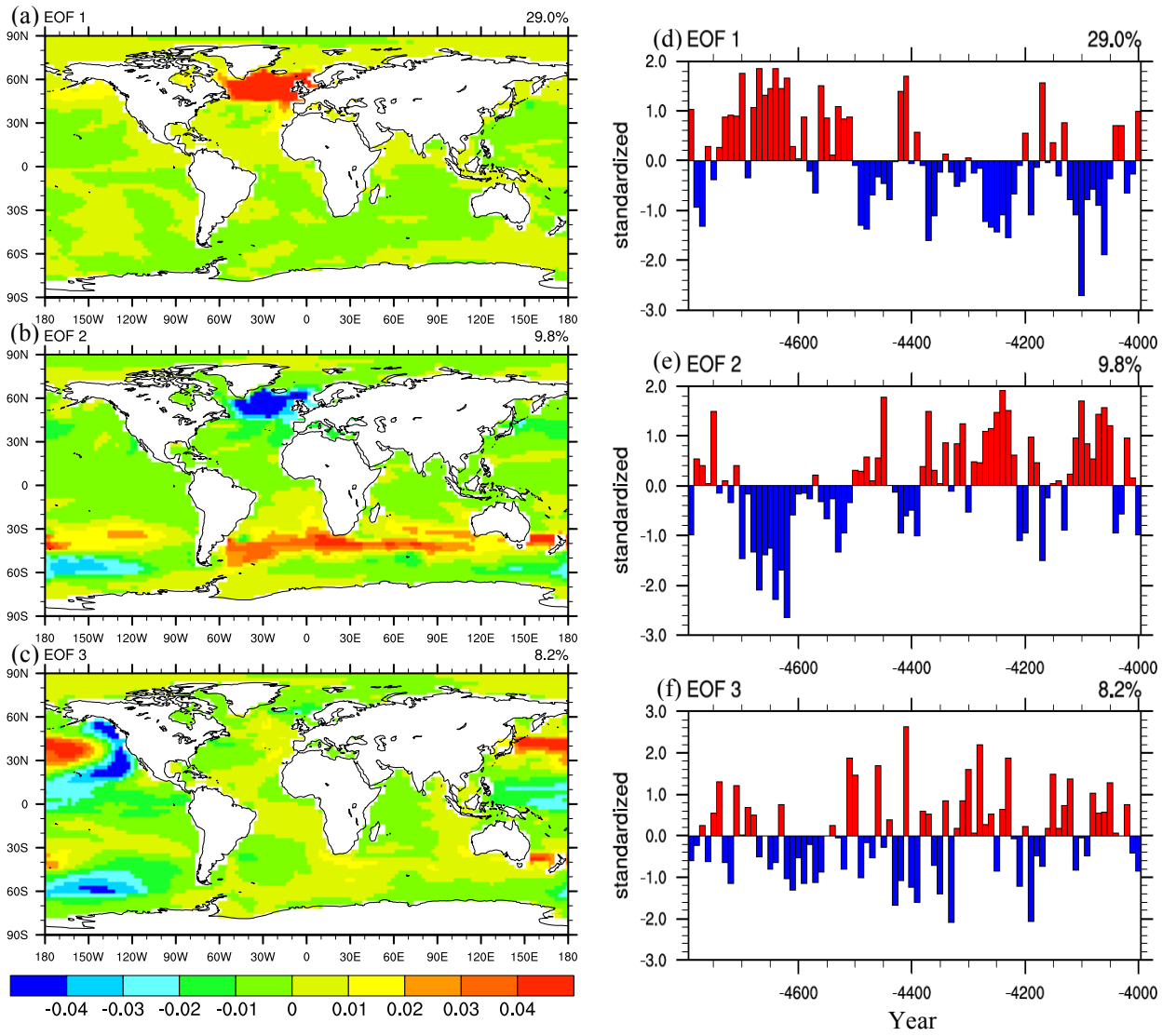

Figure 3. The first three patterns (a-c) and principal components (d-f) of rotated EOF modes on the SST over the period 4800-4000ka BP.

512
513

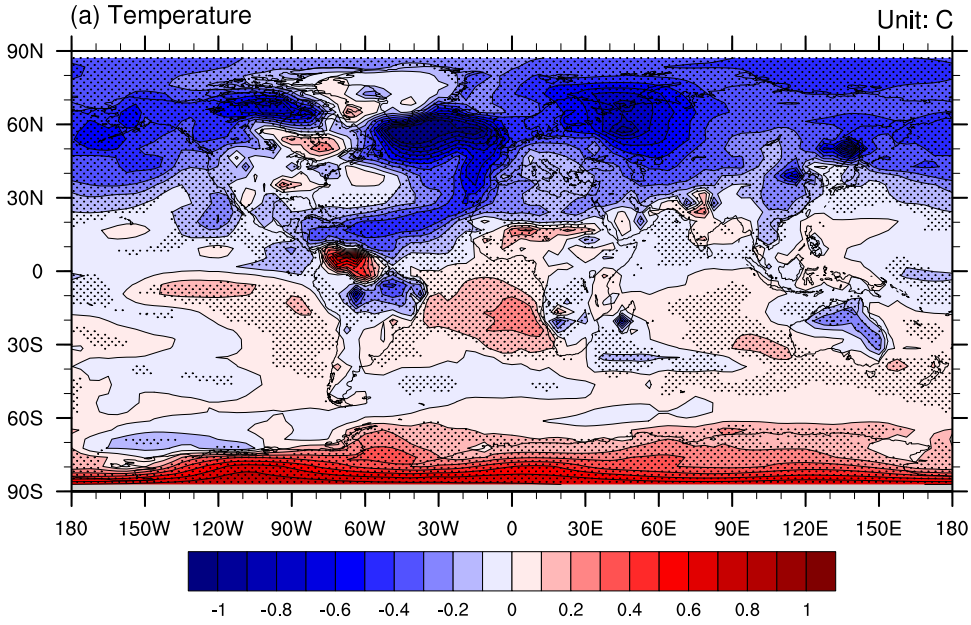

514

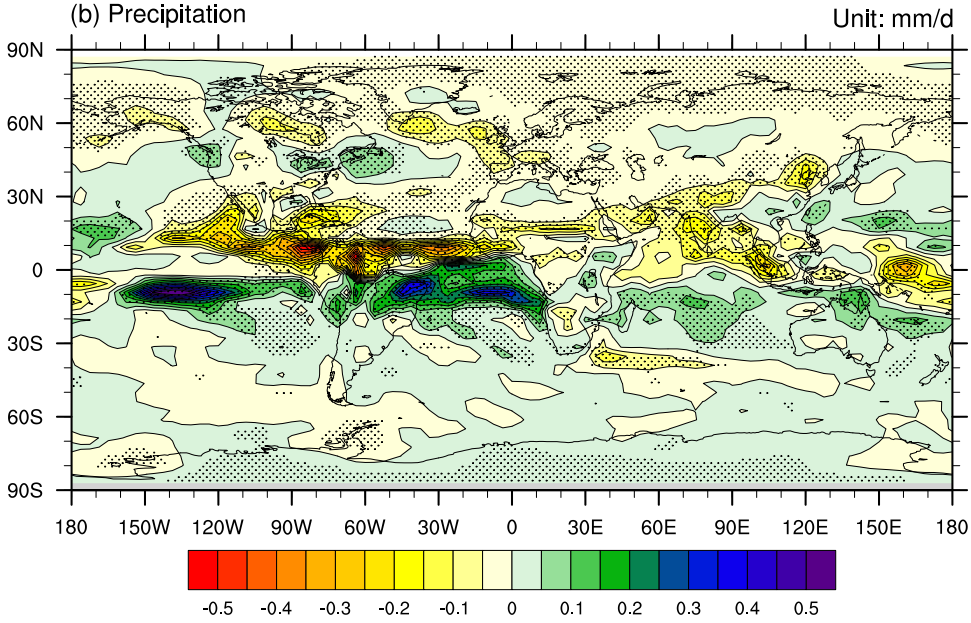

515

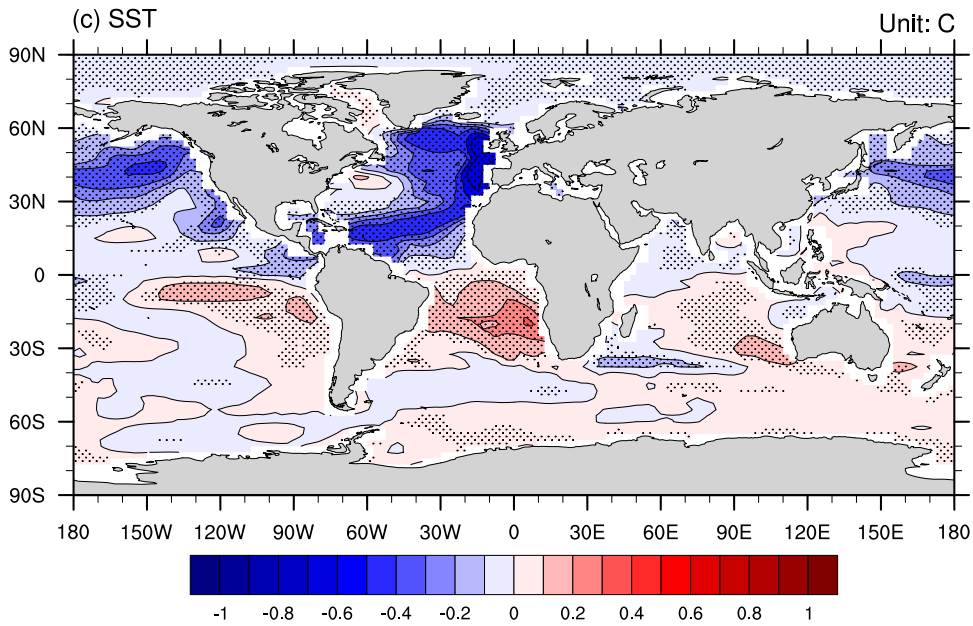

Figure 4. The changes of (a) surface temperature (°C), (b) precipitation (mm/day), and (c) SST (°C) after 8.8ka BP (between 8800-8000ka BP and 9200-8800ka BP)

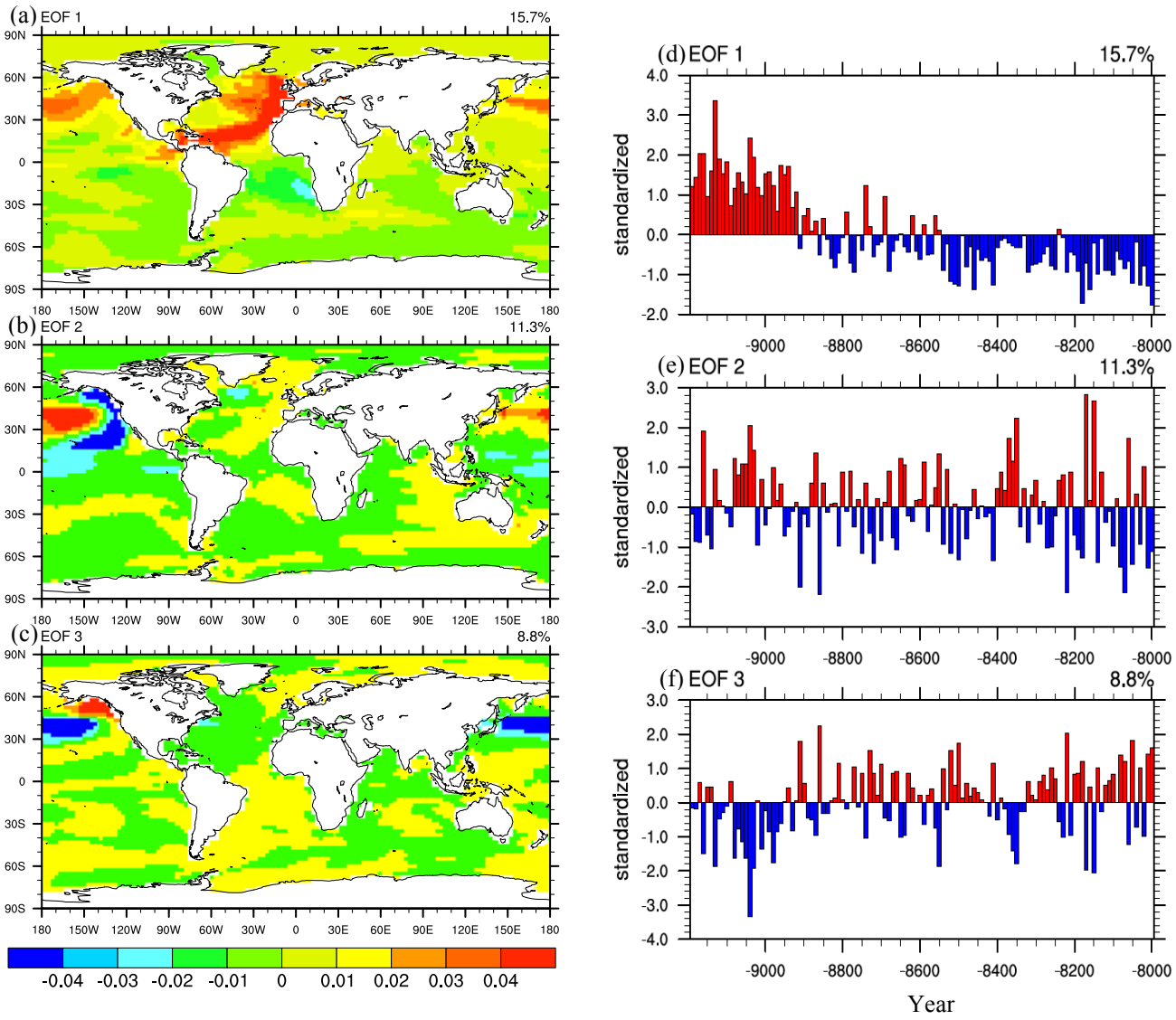

Figure 5. The first three patterns (a-c) and principal components (d-f) of rotated EOF modes on the SST over the period 9200-8000ka BP.

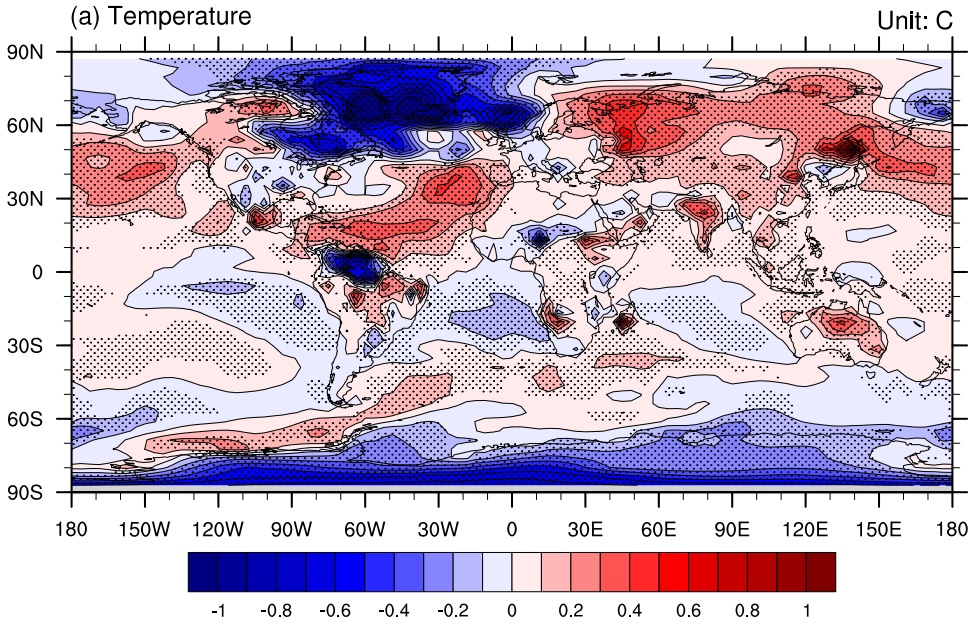
(a) Temperature
Unit: C
90N
60N
30N
0
30S
60S
90S
180 150W 120W 90W 60W 30W 0 30E 60E 90E 120E 150E 180
-1 -0.8 -0.6 -0.4 -0.2 0 0.2 0.4 0.6 0.8 1

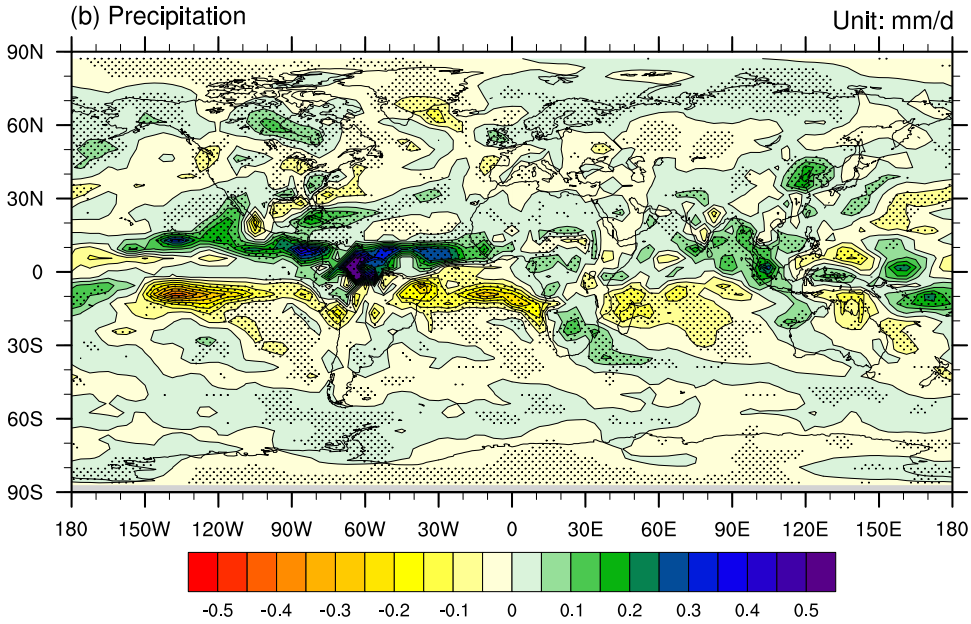
(b) Precipitation
Unit: mm/d
90N
60N
30N
0
30S
60S
90S
180 150W 120W 90W 60W 30W 0 30E 60E 90E 120E 150E 180
-0.5 -0.4 -0.3 -0.2 -0.1 0 0.1 0.2 0.3 0.4 0.5

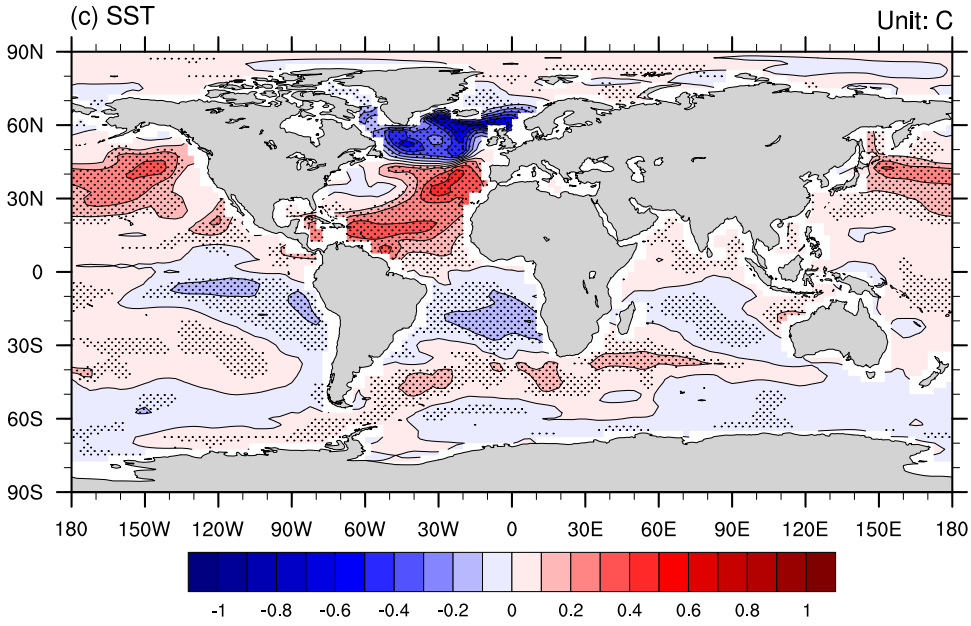

Figure 6. The differences between changes of (a) surface temperature (°C), (b) precipitation (mm/day), and (c) SST (°C) of the 5th millennium BP and 9th millennium BP periods shown in Figures 2 and 4.

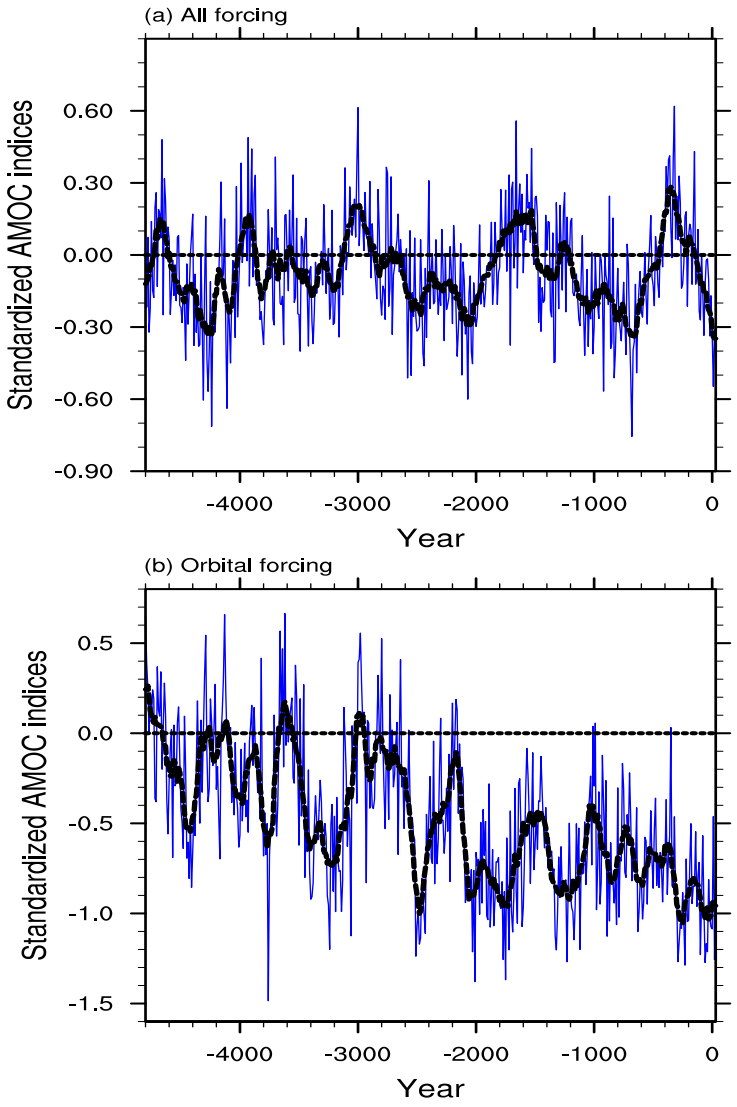

608

609 **Figure 7.** The 10-year running averaged (blue line) and 100-year running averaged (black line)
610 time series of AMOC strength, plotted as anomalies from the mean for 4800-4500 years B.P. from
611 (a) all-forcing experiment and (b) orbital-forcing experiment. AMOC strength was below the mean
612 for 63% of the time in the all-forcing experiment and 87% of the time in the orbital-forcing
613 experiment.

614

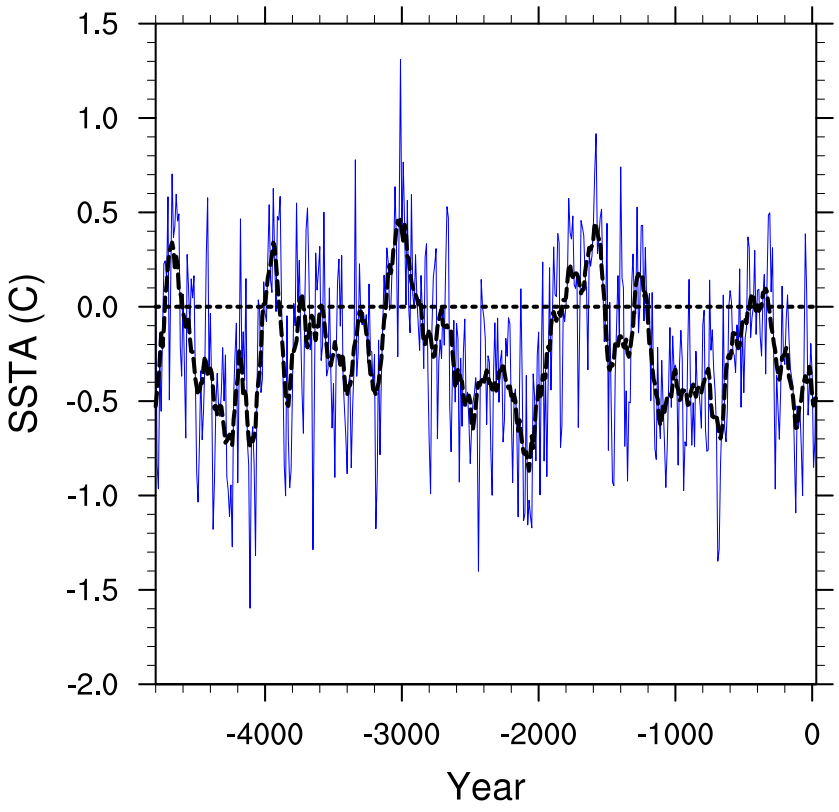

Figure 8. The 10-year running averaged (blue line) and 100-year running averaged (black line) SSTs in the area of the North Atlantic with significant negative SST differences between the 5th millennium BP and 9th millennium BP periods (40-60 °N, 7.5-60 °W) on Figure 2c, plotted as anomalies from the mean for 4800-4500 years B.P. ~69% of the time, temperatures in this region were below the mean.